J Comput Electron (2006) 5:155–159
DOI 10.1007/s10825-006-8836-z

A fast and stable Poisson-Schrödinger solver for the analysis of carbon nanotube transistors

M. Pourfath · H. Kosina · S. Selberherr

Abstract When the coupled Schrödinger-Poisson system is solved iteratively with appropriate numerical damping, convergence problems are likely to occur. We show that these problems are due to inappropriate energy discretization for evaluating the carrier concentration. By using an adaptive method the self-consistent loop becomes stable, and most of the simulations converge in a few iterations. We applied this approach to investigate the behavior of carbon nanotube field effect transistors.

Keywords Nanotube field-effect transistor · Convergence · Adaptive grid

1. Introduction

As electronic devices shrink the carrier transport through these devices is more affected by quantum mechanical phenomena, implying the need for coupled Schrödinger-Poisson solvers to analyze these devices. Non-linear coupled systems can be solved by iteration with appropriate numerical damping, which terminates if a convergence criterion is satisfied [1]. However, convergence problems of the coupled Schrödinger-Poisson system are well known [2]. Rigorous analysis of this system suggests that instabilities are due to inappropriate energy discretization for evaluating the carrier concentration. Conventionally the energy domain is discretized on an equidistant grid to solve the Schrödinger equation and evaluate the carrier concentration. The disadvantage of this method is that the accuracy of the calculated quantity can not be predefined and in fact it is problem-dependent. As will be shown, inaccurate carrier concentration in the self-consistent loop causes instabilities. By using an adaptive integration method with predefined accuracy a fast and stable solver is achieved.

Exceptional electronic and mechanical properties together with nanoscale diameter make carbon nanotubes (CNTs) candidates for nanoscale field effect transistors (FETs). While early devices have shown poor device characteristics, high performance devices were achieved recently [3–6]. In short CNTs (less than 100 nm) the carrier transport is nearly ballistic [5, 7]. Depending on the work-function of the metal contact positive, zero, or negative barrier height at the metal-CNT interface is formed [8, 9]. The barrier height for electrons is defined as the energy difference between the Fermi level in the contact and the conduction band-edge of the CNT. To investigate the behavior of CNTFETs with different barrier heights we solve the coupled Poisson and Schrödinger equation.

2. Approach

In order to account for the ballistic transport we solved the coupled Poisson and Schrödinger equations for CNTFETs.

$$\frac{\partial^2 V}{\partial \rho^2} + \frac{1}{\rho}\frac{\partial V}{\partial \rho} + \frac{\partial^2 V}{\partial z^2} = -\frac{Q}{\epsilon} \tag{1}$$

$$-\frac{\hbar^2}{2m^*}\frac{\partial^2 \Psi_{s,d}^{n,p}}{\partial z^2} + (U^{n,p} - E)\Psi_{s,d}^{n,p} = 0 \tag{2}$$

We considered an azimuthal symmetric structure, in which the gate surrounds the CNT, such that the Poisson Eq. (1) is restricted to two-dimensions. In (1) $V(\rho, z)$ is the elec-

M. Pourfath (✉) · H. Kosina · S. Selberherr
Institute for Microelectronics, Technische Universität Wien,
Gußhausstraße 27–29, A-1040 Wien, Austria
e-mail: pourfath@iue.tuwien.ac.at

trostatic potential, and Q is the space charge density. In the Schrödinger Eq. (2) the effective mass is assumed to be $m^* = 0.05\mathrm{m}_0$ for both electrons and holes [10]. In (2) superscripts denote the type of the carriers. Subscripts denote the contacts, where s stands for the source contact and d for the drain contact. For example, Ψ_s^n is the wave function associated with electrons that have been injected from the source contact, and U^n is the potential energy that is seen by electrons. The Schrödinger equation is just solved on the surface of the tube, and is restricted to one-dimension because of azimuthal symmetry. The space charge density in (1) is calculated as:

$$Q = \frac{q(p-n)\delta(\rho-\rho_{cnt})}{2\pi\rho_{cnt}} \tag{3}$$

where q is the electron charge, and n and p are total electron and hole concentrations per unit length. In (3) δ/ρ is the Dirac delta function in cylindrical coordinates, implying that carriers were taken into account by means of a sheet charge distributed uniformly over the surface of the CNT [11]. Including the source and drain injection components, the total electron concentration in the CNT is calculated as:

$$\begin{aligned} n &= \frac{4}{2\pi}\int f_s|\Psi_s^n|^2 dk_s + \frac{4}{2\pi}\int f_d|\Psi_d^n|^2 dk_d \\ &= \int \frac{\sqrt{2m^*}}{\pi\hbar\sqrt{E_s}} f_s|\Psi_s|^2 dE_s + \int \frac{\sqrt{2m^*}}{\pi\hbar\sqrt{E_d}} f_d|\Psi_d|^2 dE_d \end{aligned} \tag{4}$$

where $f_{s,d}$ are equilibrium Fermi functions at the source and drain contacts. All our calculations assume a CNT with 0.6 eV band gap [3]. The total hole concentration in the CNT is calculated analogously.

The Landauer-Büttiker formula [12] is used for calculating the current:

$$I^{n,p} = \frac{4q}{h}\int \left[f_s^{n,p}(E) - f_d^{n,p}(E)\right] TC^{n,p}(E)dE \tag{5}$$

where $TC^{n,p}(E)$ are the transmission coefficients of electrons and holes, respectively, through the device. The factor 4 in (4) and (5) stems from the twofold band and twofold spin degeneracy.

The coupled Schrödinger and Poisson equation system was solved iteratively [1], by using an appropriate numerical damping factor α. At the $(k+1)$th iteration the Schrödinger equation is solved using the electrostatic potential V^k from the last iteration and the new space charge density Q^{k+1} is calculated. The Poisson equation is then solved by using Q^{k+1} and an intermediate new electrostatic potential is calculated V_{int}^{k+1}. Finally V^{k+1} is calculated as:

$$V^{k+1} = \alpha V_{\mathrm{int}}^{k+1} + (1-\alpha)V^k \tag{6}$$

where $0 < \alpha < 1$. Successive iteration continues until a convergence criterion is satisfied. In this work an adaptive damping factor was used [13]. The damping factor is initially set to $\alpha = 1$. If the the potential update $|V^{k+1} - V^k|$ increases from one iteration to the next iteration or remains constant the the damping factor decreases by a constant factor.

The integration in (4) is calculated within an energy interval $[E_{\min}, E_{\max}]$. The interval can be simply divided into equidistant steps and the Schrödinger equation will be solved at these points. By using this method narrow resonances at some energies may be missed or may not be evaluated correctly. In successive iterations as the potential profile changes the position of the resonances will also change, and it is possible that a resonance point locates very near to one of the energy steps. In this case the carrier concentration suddenly changes and as a result the simulation would oscillate and not converge. To avoid this problem the accuracy of the integration should be independent of the location of resonances. By using an adaptive integration method the integrations in (4) can be evaluated with a desirable accuracy. Assume f is an integrable function, and $[a, b]$ is the interval of integration. To compute

$$I = \int_a^b f(x)dx \tag{7}$$

adaptively I is calculated with two different integration methods, I_1 and I_2. If the relative difference of the two approximations is less than a predefined tolerance the integration is accepted, otherwise the interval $[a, b]$ is divided into two equal parts $[a, c]$ and $[c, b]$, where $c = (a+b)/2$, and the two respective integrals are computed independently.

$$I = \int_a^c f(x)dx + \int_c^b f(x)dx \tag{8}$$

The same procedure is performed for each of these integrals. The advantage of this methods is that the steps are non-equidistant, so there are many points around the resonances while in other regions there are few points. In this work an adaptive Simpson quadrature [14] is used. In this method the two successive Simpson approximates are calculated:

$$I_1 = \frac{h}{6}(f(a) + 4f(c) + f(b)) \tag{9}$$

$$I_2 = \frac{h}{12}(f(a) + 4f(d) + 2f(c) + 4f(e) + f(b)) \tag{10}$$

where $d = (a+c)/2$, and $e = (c+b)/2$. If $|I_1 - I_2| \leq \mathrm{tol} \times |I_2|$ the integration is evaluated within one step

of Romberg extrapolation: $I = I_2 + (I_2 - I_1)/15$. A value of $\text{tol} > 10^{-2}$ results in an instability of the self-consistent loop, whereas a smaller value increases the simulation time. Our simulation results show that $\text{tol} = 5 \times 10^{-3}$ is an appropriate value for this parameter.

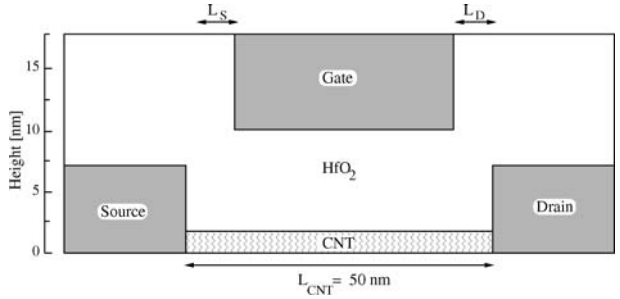

Fig. 1 Sketch of the cylindrical device

3. Simulation results

To investigate adaptive and non-adaptive methods in more detail, we performed simulations of the CNTFET shown in Fig.1. The band-edge profile along the device is shown in Fig. 2(a). Figure 2(b) shows the carrier concentration calculated by adaptive and non-adaptive methods. By increasing the number of points in the non-adaptive method, the calculated carrier concentration becomes more accurate and reaches the value achieved from adaptive method. The reason of such large differences is the existence of narrow resonances at certain energies. Figure 2(c) shows the transmission probability of carriers through the device. The resonances result from confined states in the device, at which the carrier concentration peaks. Figure 2(d) shows the first resonance in more detail. Non-adaptive methods miss the proper shape of

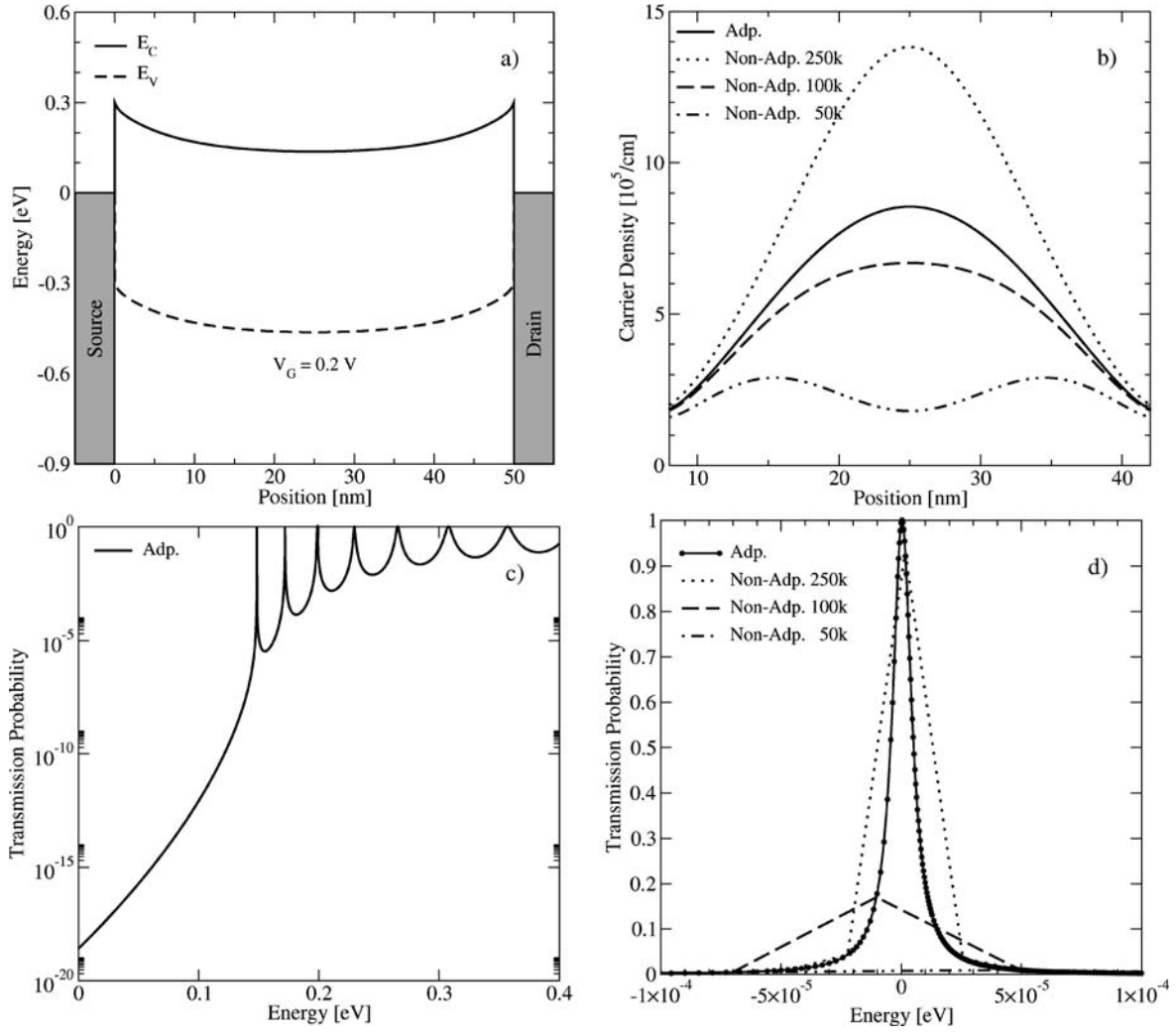

Fig. 2 Simulation results at $V_G = 0.2V$ and $V_D = 0.0V$. (a) Band edge profile along the device. (b) Comparison of achieved carrier concentration from the adaptive and non-adaptive methods. (c) Transmission probability of carriers through the device calculated by the adaptive method. (d) The first resonance of the transmission probability in more detail (the peak energy is shifted to zero). Non-adaptive methods miss the peak while the adaptive method capture the right shape of the resonance

the resonance and as a result they are not able to calculate the carrier concentration accurately. The advantage of the adaptive method is that the grid spacing is non-uniform and more points are generated near the resonances. With the adaptive method, for an accuracy of 1.0×10^{-2} about 8.5×10^{2} grid points were required, while with the non-adaptive method even with 2.5×10^{5} grid points the accuracy is not satisfactory.

Inaccuracy in the calculation of the carrier concentration will lead to instabilities of the self-consistent loop. Figure 3(a) shows the norm of the potential update after each iteration for the adaptive and non-adaptive methods. By increasing the number of points in the non-adaptive method the accuracy of the calculated carrier concentration increases and as a result the stability of the self-consistent loop improves. But by increasing the number of points the simulation time increases greatly (Fig. 3(b)). Compared to the non-adaptive method, the adaptive method is more stable due to accurate quantity calculations and less CPU-time demanding due to a relatively low total number of points.

We applied this methodology to investigate the behavior of the CNTFET shown in Fig. 1. The transfer and output characteristics for devices with different barrier heights for electrons are shown in Fig. 4(a) and (b). The ambipolar behavior is clearly observed, especially for the device with positive barrier heights. Geometrical changes for suppressing this phenomenon is reported in [15]. Simulation results suggest that by reducing the barrier height for one carrier type, here for electrons, the ambipolar behavior is reduced

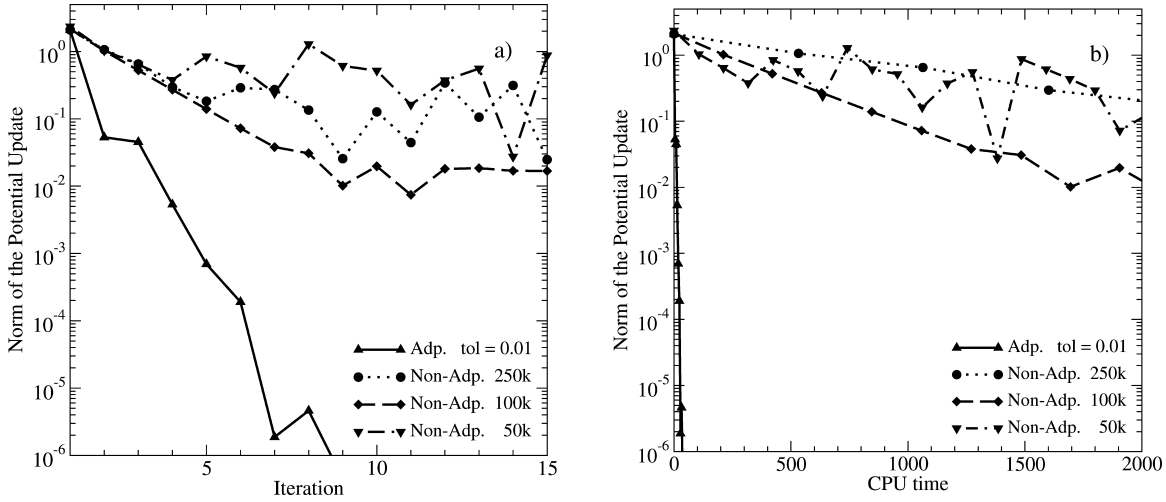

Fig. 3 (a) The norm of the potential update after each iteration for adaptive and non-adaptive methods. (b) The norm of the potential update versus CPU time for adaptive and non-adaptive methods. The simulations were performed on an IBM-RS6000

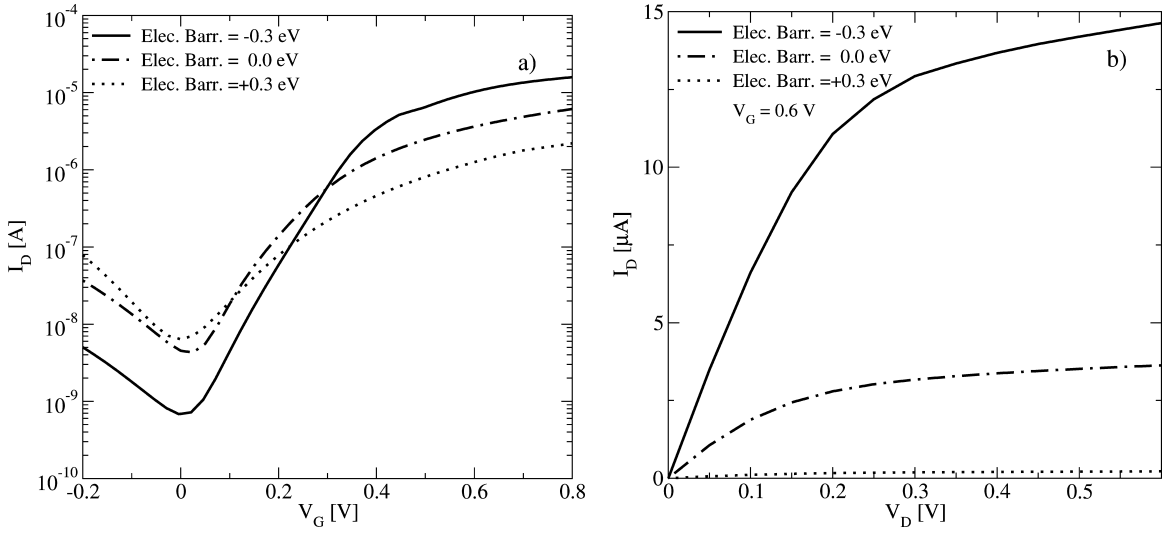

Fig. 4 (a) Transfer characteristics, and (b) output characteristic of CNTFETs with different barrier heights for electrons

and the on-current increases, which is favorable for device characteristics.

4. Conclusions

We showed that by using an adaptive integration method the iterative solution of the coupled Poisson and Schrödinger system will be more stable and less CPU-time demanding. We used this method to investigate the behavior of CNTFETs with different barrier heights. Simulation studies indicate that in order to improve the device characteristics the barrier height for one carrier type at the metal-CNT interface should be reduced. The implemented solver can be used for optimization of CNTFETs.

Acknowledgments This work was partly supported by the European Commission, contract No. 506844 SINANO.

References

1. Stern, F.: Phys. stat. sol. (b) **6**, 56 (1970)
2. Trellakis, A., Galick, A.T., Pacelli, A., Ravaioli, U.: J. Appl. Phys. **81**, 7880 (1997)
3. Radosavljevic, M., Appenzeller, J., Avouris, P., Knoch, J.: Appl. Phys. Lett. **84**, 3693 (2004)
4. Kim, B.M., Brintlinger, T., Cobas, E., Zheng, H., Fuhrer, M., Yu, Z., Droopad, R., Ramdani, J., Eisenbeiser, K.: Appl. Phys. Lett. **84**, 1946 (2004)
5. Javey, A., Guo, J., Farmer, D.B., Wang, Q., Yenilmez, E., Gordon, R.G., Lundstrom, M., Dai, H.: Nano Lett. **4**, 1319 (2004)
6. Javey, A., Tu, R., Farmer, D.B., Guo, J., Gordon, R.G., Dai, H.: Nano Lett. **5**, 345 (2005)
7. Javey, A., Guo, J., Wang, Q., Lundstrom, M., Dai, H.: Letters to Nature **424**, 654 (2003)
8. Appenzeller, J., Radosavljevic, M., Knoch, J., Avouris, P.: Phys. Rev. Lett. **92**, 048301 (2004)
9. Guo, J., Datta, S., Lundstrom, M.: IEEE Trans. Electron Devices **51**, 172 (2004)
10. Saito, R., Dresselhaus, G.D., Dresselhaus, M.S.: Physical properties of carbon nanotubes. (Imperial College Press (1998)
11. John, D., Castro, L., Pereira, P., Pulfrey, D.: In Proc. NSTI Nanotech (2004) vol. **3**, pp. 65–68
12. Datta, S.: Electronic transport in mesoscopic systems. (Cambridge University Press (1995)
13. Kerkhoven, T., Galick, A.T., Ravaioli, U., Arends, J.H., Saad, Y.: J. Appl. Phys. **68**, 3461 (1990)
14. Lyness, J.N.: J. ACM **16**, 483 (1969)
15. Pourfath, M., Ungersboeck, E., Gehring, A., Cheong, B.H., Park, W., Kosina, H., Selberherr, S.: In Proc. ESSDERC (2004) pp. 429–432